Selective hydrogenation of acrolein over Pd model catalysts: temperature and particle size effects

Casey P. O'Brien[a], Karl-Heinz Dostert[a], Swetlana Schauermann[a,b]*, and Hans-Joachim Freund [a]

[a]Department of Chemical Physics, Fritz-Haber-Insitut der Max-Planck Gesellschaft, 14195 Berlin, Germany

[a]Institute of Physical Chemistry, Christian-Albrechts-University Kiel, Max-Eth-Str. 2, 24118 Kiel, Germany

*Corresponding author. E-mail address: schauermann@fhi-berlin.mpg.de

Abstract

In this work, the selectivity in hydrogenation of acrolein over Fe_3O_4-supported Pd nanoparticles is investigated as a function of nanoparticle size in the 220-270 K temperature range. While Pd(111) shows nearly 100% selectivity towards the desired hydrogenation of the C=O bond to produce propenol, Pd nanoparticles were found to be much less selective towards this product. *In-situ* detection of surface species using infrared-reflection absorption spectroscopy shows that the selectivity towards propenol critically depends on the formation of an oxopropyl spectator species. While an overlayer of oxopropyl species is effectively formed on Pd(111) turning the surface highly selective for propenol formation, this process is strongly hindered on Pd nanoparticles by acrolein decomposition resulting in CO formation. We show that the extent of acrolein decomposition can be tuned by varying the particle size and the reaction temperature. As a result, significant production of propenol is observed over 12 nm Pd nanoparticles at 250 K, while smaller (4 and 7 nm) nanoparticles did not produce propenol at any of the temperatures

1

investigated. The possible origin of particle size dependence of propenol formation is discussed.

This work demonstrates that the selectivity in hydrogenation of acrolein is controlled by the

relative rates of acrolein partial hydrogenation to oxopropyl surface species and of acrolein

decomposition, which has significant implications for rational catalyst design.

1. Introduction

Selective hydrogenation of α,β-unsaturated ketones and aldehydes, a class of compounds which have conjugated C=C and C=O bonds, is a fundamentally interesting problem and an industrially important reaction. The unsaturated alcohol produced from selective hydrogenation of the C=O bond is the desired product for the fine chemicals and pharmaceuticals industries, but thermodynamics favors hydrogenation of the C=C bond.[1] Therefore, selective hydrogenation of the C=O bond requires manipulation of the relative rates of hydrogenation by catalyst design. However, a lack of fundamental understanding of the parameters governing the selectivity and activity has inhibited the development of practical heterogeneous catalyst systems that can hydrogenate the C=O bond in α,β-unsaturated ketones and aldehydes with high selectivity and activity.

It is generally believed that the adsorption geometry of the reactant on the catalyst surface is an important factor governing the selectivity of α,β-unsaturated ketone hydrogenation[2] The adsorption geometry of the α,β-unsaturated ketone can be manipulated in favor of C=O bond hydrogenation by adding bulk substituents to the C=C functional group.[1, 2b, 3] Acrolein is the most difficult α,β-unsaturated aldehyde to selectively hydrogenate the C=O bond because there are no substituents protecting to the C=C group. Higher partial pressures of the reactant have also been shown to enhance the selectivity towards C=O bond hydrogenation.[1, 2d-f] This effect was suggested to arise from increasing surface coverage, which causes the C=C group to become more tilted with respect to the surface and less vulnerable to attack by surface hydrogen atoms.[2c, 2e, 4] The structure of the catalyst also critically influences the adsorption geometry of the reactant, and the selectivity of hydrogenation of α,β-unsaturated ketones. How particularly

the catalyst structure influences the selectivity is much less understood, than the effects of the reactant molecular structure on selective hydrogenation.

Our recent work[5] with Pd model catalysts under well-defined ultra-high vacuum conditions has given some new insight into the relationship between catalyst structure and selectivity in partial hydrogenation of acrolein. We showed for the first time that a near 100% selectivity towards hydrogenation of C=O in acrolein is possible over Pd(111). This was a particularly surprising result because Pd is a very active C=C bond hydrogenation catalyst and on powdered Pd-catalysts exhibit nearly 100% selectivity towards hydrogenation of C=C in α,β-unsaturated ketones, even when bulky protecting substituents are attached to the C=C bond.[6] Prior to our discovery, Au and Ag were the best known monometallic catalysts for selective hydrogenation of the C=O bond in acrolein, with selectivities of only ~50% [2f, 7]. However, we showed that the clean Pd(111) surface was not active for C=O bond hydrogenation, but required activation by the deposition of an oxopropyl spectator species at the beginning of the reaction. In contrast to Pd(111), model supported Pd nanoparticles showed no propenol formation, in agreement with the literature reports on powdered Pd catalysts. We observed a near 100% selectivity towards hydrogenation of the C=C bond in acrolein over Pd/Fe_3O_4. This is surprising because the investigated model Pd nanoparticles are composed of ~80% (111) facets, and are therefore very similar in structure to Pd(111), yet they exhibit much different selectivity. The differences in the selectivity of Pd nanoparticles versus Pd(111) can be related to the presence of low-coordinated sites, such as edges and corners, that seem to critically affect the selectivity of a reaction.

In this work, the influence of Pd nanoparticle structure, i.e. particle size, and the reaction conditions on selectivity in hydrogenation of acrolein is investigated. We show that there is a

strong influence of both the Pd nanoparticle size and the temperature on the selective

hydrogenation of acrolein. In general, Pd nanoparticles are much less selective towards propenol

formation because acrolein decomposes strongly on the Pd nanoparticles and hinders the

formation of oxopropyl spectator species. However, the biggest investigated Pd nanoparticles

exhibiting large fraction of (111) facets were found to produce a significant amount of propenol

in a narrow temperature range around 250 K. In contrast, over smaller nanoparticles, no

propenol formation was observed. The underlying mechanisms for this strongly structure- and

temperature-dependent selectivity are discussed.

2. Experimental

All experiments were performed at the Fritz Haber Institute with an ultra-high vacuum

molecular beam machine that has been described in detail previously.[8] Molecular beams of

acrolein and H_2 were focused on the sample simultaneously while the sample was held at a

constant temperature. The effusive molecular beams were produced by doubly differentially

pumped multi-channel array sources. Acrolein (Sigma-Aldrich, 95% purity) was purified prior

to each experiment by repeated freeze-pump-thaw cycles. During all reactivity experiments the

flux of H_2 on the sample surface was 4.8×10^{15} molecules/cm^2/s. The sample was exposed to H_2

for five minutes prior to acrolein exposure. The flux of acrolein on the sample surface was

1.5×10^{13} molecules/cm^2/s during pulsed reactivity experiments and 0.6×10^{13} molecules/cm^2/s

during continuous reactivity experiments. Gas-phase fragments related to acrolein (parent ion at

56 a.m.u.), H_2: (2 a.m.u.), propanal (parent ion and main fragment at 58 a.m.u.), propenol (parent

ion at 58 a.m.u., main fragment at 57 a.m.u. and further prominent fragment at 31 a.m.u.),

propanol (parent ion at 60 a.m.u., main fragment at 31 a.m.u.) were detected with a quadrupole

mass spectrometer (ABB Extrel). Simultaneously, surface species were detected using a Bruker

IFS 66v infrared spectrometer with an MCT detector and a spectral resolution of 2 cm^{-1}.

The method for preparing the Pd/Fe$_3$O$_4$ model catalysts has been described in detail

previously.[9] Briefly, a well-ordered ~10 nm thick Fe$_3$O$_4$ film was grown on a Pt(111) substrate

(see references [10] for details) followed by Pd deposition onto the Fe$_3$O$_4$ film at 120 K by

physical vapor deposition of Pd (Goodfellow, >99.9%) using a commercial evaporator (Focus

EFM 3). After depositing Pd, the sample was annealed at 600 K and the Pd nanoparticles were

stabilized by repeated cycles of oxidation and reduction at 500 K.[11] The size of the Pd

nanoparticles was controlled by the nominal thickness of the Pd film deposited onto the Fe$_3$O$_4$

substrate at 120 K (see reference [9] for details). The Pd(111) crystal was cleaned by repeated

cycles of Ar$^+$ sputtering at room temperature, annealing at 1000 K, and oxidation in 1x10^{-6} mbar

O$_2$ at 750 K. The cleanliness of the Pd/Fe$_3$O$_4$ and Pd(111) samples was verified prior to every

experiment by IRAS of adsorbed CO.

3. Results and Discussion

3.1. Influence of Pd particle size and temperature on activity and selectivity

Acrolein hydrogenation was performed over Pd(111) and Fe$_3$O$_4$-supported Pd

nanoparticles with varying particle sizes (4 nm, 7 nm, 12 nm) at three different temperatures

(220 K, 250 K, 270 K) to investigate the influence of Pd structure and surface temperature on its

activity and selectivity for hydrogenation of acrolein. A continuous beam of H$_2$ was focused on

the sample surface, which was held at constant temperature, for five minutes prior to the

introduction of acrolein to saturate the surface with hydrogen. Thereafter a molecular beam of

acrolein was exposed to the sample in six second pulses (six seconds on, six seconds off) while

the product gas was analyzed with a quadrupole mass spectrometer. Figure 1 shows the

formation rates of propenol (left column) and propanal (right column) over Pd(111) and

Pd/Fe$_3$O$_4$ model catalysts with varying Pd particle size (4 nm, 7 nm, and 12 nm) at 220 K (top

row), 250 K (middle row), and 270 K (bottom row). The obtained reaction rates show a strong

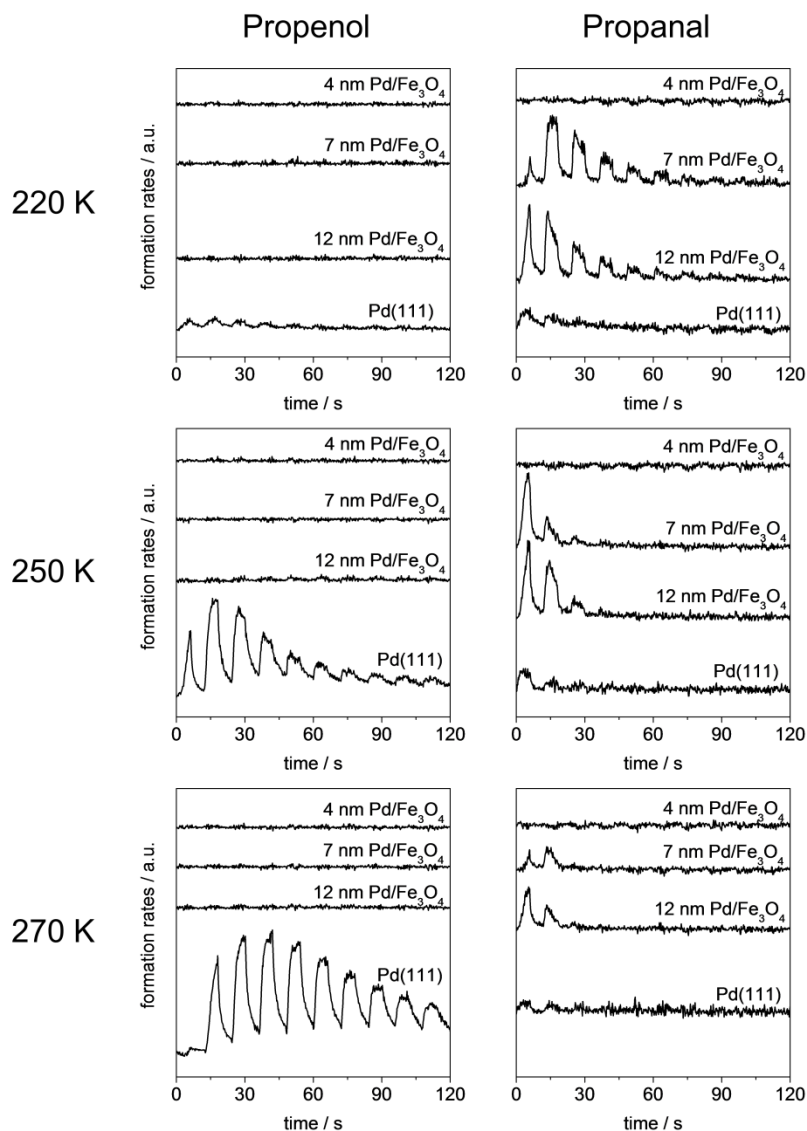dependence on the Pd structure and temperature.

Figure 1. *Gas-phase formation rates of propenol (left column) and propanal (right column) over Pd(111) and model Pd nanoparticles supported on Fe$_3$O$_4$ model catalysts with average Pd*

nanoparticle size 4, 7, and 12 nm at 220 K (top row), 250 K (middle row), and 270 K (bottom row).

On Pd nanoparticles, there was no significant propenol production in the 4-12 nm particle size range and in the 220-270 K temperature range. Propanal production was observed over both the 7 nm and the 12 nm Pd particles at similar rates at all three temperatures, and were significantly higher than the rates of propanal production over Pd(111). The rate of propanal production is highest at 220 K and decreases with increasing temperature. The 4 nm Pd particles did not produce a significant amount of either propenol or propanal in the entire 220-270 K temperature range. The total concentration of Pd atoms on the 4 nm Pd/Fe_3O_4 catalyst is more than an order-of-magnitude less than that on the 7 nm Pd/Fe_3O_4 and 12 nm Pd/Fe_3O_4 catalysts and, therefore, it is likely that the concentration of Pd atoms is too low to produce a significant amount of reaction products. These results are in agreement with numerous literature studies reporting essentially exclusive formation of propanal over Pd nanoparticles in powdered catalysts.[3, 12]

In contrast to Pd nanoparticles, significant propenol production was observed over Pd(111), and the amount of propenol produced increased from almost zero at 220 K to a maximum at 270 K. The Pd(111) catalyst also produced a small amount of propanal at all three temperatures. The amount of propanal produced over Pd(111) was similar to that of propenol at 220 K. However, the selectivity towards propenol production increased with increasing temperature, and at 270 K, the Pd(111) catalyst was nearly 100% selective towards production of propenol.

These results indicate that the selectivity in hydrogenation of acrolein is dependent on both the Pd structure and on the reaction temperature. While the Pd nanoparticles are 100%

8

selective towards production of propanal, the Pd(111) catalyst is highly selective towards propenol production. The reaction temperature also strongly affects the selectivity since the maximum rate of propanal production is observed at 220 K whereas the maximum rate of propenol production is observed at 270 K. Obviously, the selectivity in hydrogenation of acrolein can be tuned by controlling both the Pd nanoparticle size and the reaction temperature.

3.2. Mechanism of hydrogenation to propenol on Pd(111)

To understand the underlying mechanisms that are responsible for the strong structure- and temperature-dependence displayed in both the activity and selectivity of acrolein hydrogenation, IRAS was performed to identify and monitor the species formed on the surface in the course of the reaction. The Pd model catalysts were continuously exposed to molecular beams of H_2 and acrolein while surface species and gas-phase products were detected simultaneously with IRAS and mass spectrometry, respectively.

We begin by analyzing the mechanism of acrolein hydrogenation over Pd(111) at 270 K, which are the conditions that resulted in the highest activity and selectivity towards propenol production. Figure 2(a) displays the gas-phase production rates of propenol and propanal over Pd(111) during continuous exposure to acrolein and H_2 at 270 K. The results displayed in Figure 2(a) are similar to those obtained during pulsed reactivity experiments under similar conditions (Figure 1). Following an induction period of ~20 seconds at the beginning of the reaction, in which there was no gas-phase products formed, the rate of propenol production increases sharply to a maximum at about 90 seconds and then decreases slowly over the next 270 seconds. Production of propanal was negligible over the course of the entire reaction and, following the induction period, Pd(111) exhibited a near 100% selectivity towards propenol production.
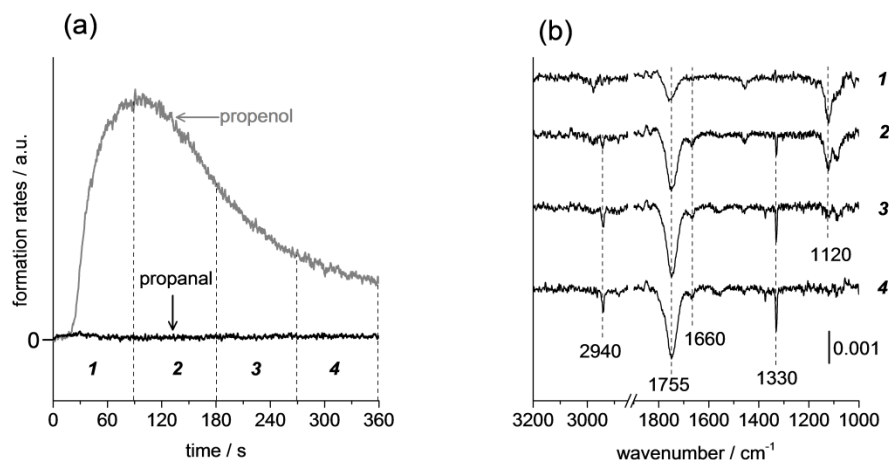
9

Figure 2. Acrolein hydrogenation over Pd(111) at 270 K. (a) Gas-phase formation rates of propanal (black) and propenol (grey). (b) Time-resolved IRAS spectra collected during acrolein hydrogenation over Pd(111) at 270 K. Spectra labeled 1-4 were collected during the regions labeled 1-4 in (a).

The induction period at the beginning of the reaction suggests that the clean Pd(111) surface is not active for propenol production, and Pd(111) must accumulate acrolein derivatives prior to the formation of propenol begins. By knowing precisely the acrolein exposure via dosing with molecular beams, we calculated that about one acrolein molecule per four surface Pd atoms was accumulated on the surface during the induction period, which results in densely packed overlayer of acrolein-derived surface species. Detection of surface species *in-situ* with IRAS provides detailed insight into the chemical composition of the surface turning over. Figure 2(b) shows the IRAS spectra collected during acrolein hydrogenation over Pd(111) at 270 K. The spectra labeled '1' through '4' in Figure 2(b) were recorded during the corresponding regions labeled in Figure 2(a). Assignment of the bands shown in Figure 2b was given in our previous work.[5a]

Three major groups of bands corresponding to different surface species can be identified. First, the band at 1755 cm^{-1} correspond to the stretching vibration of the C=O bond.[13] Note that

the C=O vibration in molecularly adsorbed acrolein, in which the C=O bond is conjugated to the C=C double bond, lies around 1660 cm^{-1}[13b, 13c]. The significantly higher frequency band at 1755 cm^{-1} suggests that the corresponding surface species contain C=O bonds, which are not conjugated to the C=C bonds.[14] The appearance of this vibration points to the formation of an oxopropyl surface species, resulting from the partial hydrogenation of acrolein molecules with only one H atom attached to the C=C bond. Figure 3 show a possible structure of the oxopropyl species. Please note that there two feasible structures of oxopropyl species: bonded to the surface via the C2-carbon as shown in Figure 3 and bonded through the terminal C3-carbon. Based on the available IRAS data, it is impossible to differentiate between these structures. Remarkably, the band at 1755 cm^{-1} already appears at a very early stage of the reaction, grows in intensity and remains intense, even after the reaction rate recorded in the gas phase vanishes. This observation strongly suggests that this species is not the reaction intermediate leading to the final gas phase product propenol, but is merely a spectator.

The second prominent band is the very intense vibration at 1120 cm^{-1}. Note that this frequency is present neither in adsorbed intact acrolein on Pd nor in acrolein ice[13a] and therefore cannot be related to any prominent vibration of the molecularly adsorbed acrolein. Further, this band appears only under reaction conditions: in the presence of H$_2$ in the temperature range 220-270 K. The most striking observation of this study is that the evolution of this vibrational band shows strong correlation with the evolution of propenol in the gas phase. Indeed, this band starts to appear in the region 1, which comprises the induction period and the region of growing reaction rate (Fig. 2a); then grows in intensity in regions of the highest reactivity 2. Consecutively, the intensity of this band strongly decreases in region 3 accompanied by the decrease of the propenol formation rate in the gas phase and completely disappears when

reactivity strongly decreases. A few other IR bands in the region of CH_x stretching and bending vibrations may also be correlated to the gas phase formation rate of propenol.[5a]

By recording IR spectra with higher time resolution, we were able to show that there is a strong correlation between the gas phase formation rate of propenol and the evolution of the vibrational band at 1120 cm^{-1}. This observation implies that the corresponding surface species is the surface intermediate, directly involved in the selective hydrogenation of the C=O bond. Taking into account all vibrational bands associated with this reaction intermediate, it is possible to identify it as a propenoxy-group CH_2=CH–CH–O····Pd, in which the C–O entity is attached to Pd through the O atom to form a single C–O····Pd bond. This intermediate can be formed though adsorption of acrolein via the C=O bond and the addition of one H atom at the C next to O. Only one additional step – the insertion of the second H atom into the Pd····O bond – is required to form propenol. Importantly, it was observed that the propenoxy reaction intermediate appears only after a densely packed overlayer of oxopropyl species was formed. This densely packed oxopropyl-overlayer creates a geometrical constraint for acrolein adsorption via the C=C bond and forces the adsorption via C=O bond thus inducing the desired selectivity.

The third prominent band appears at 1330 cm^{-1} during the period of highest reactivity and steadily grows in intensity, remaining intense even after the complete stop of the reaction. This band was previously related to formation of ethylidyne and ethylidyne-like species.[15] This species can be considered as the second type of spectator or a surface poison.

In the following sections, we show that formation of this oxopropyl species is necessary, but not sufficient, for propenol formation over Fe_3O_4-supported Pd nanoparticles.
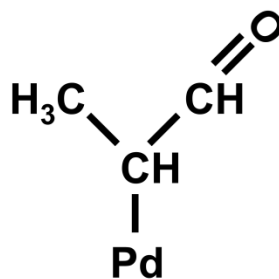
Figure 3. Possible structure of the oxopropyl spectator species that is formed from partial hydrogenation of the C=C bond in acrolein and is responsible for activating the Pd(111) surface for C=O bond hydrogenation in acrolein.

3.3. Partial hydrogenation of acrolein over Pd/Fe₃O₄ at 270 K

Although the surfaces of the Fe_3O_4-supported Pd nanoparticles are composed of ~80% (111) facets,[9] Figure 1 demonstrates that their activity and selectivity in partial hydrogenation of acrolein is vastly different than that of Pd(111). Pd nanoparticles exhibit rather low activity and are 100% selective towards hydrogenation of the C=C bond whereas Pd(111) is nearly 100% selective towards hydrogenation of the C=O bond. To understand why the Fe_3O_4-supported Pd nanoparticles behave so much differently than Pd(111), the mechanisms of acrolein partial hydrogenation over Pd/Fe_3O_4 were investigated by monitoring the formation of surface species and gas-phase products simultaneously. We begin by analyzing the mechanism of acrolein hydrogenation over 12 nm Pd particles at the sample temperature (270 K) that is optimal for propenol production over Pd(111).

Figure 4(a) shows the formation rates of propanal and propenol over 12 nm Pd particles at 270 K during continuous exposure of acrolein and H_2. As expected from the results of pulsed reactivity experiments (Figure 1), there was no significant production of propenol over the entire course of the reaction. In contrast to the induction period observed in the propenol production

over Pd(111), the rate of propanal production increases from the beginning of the reaction to a

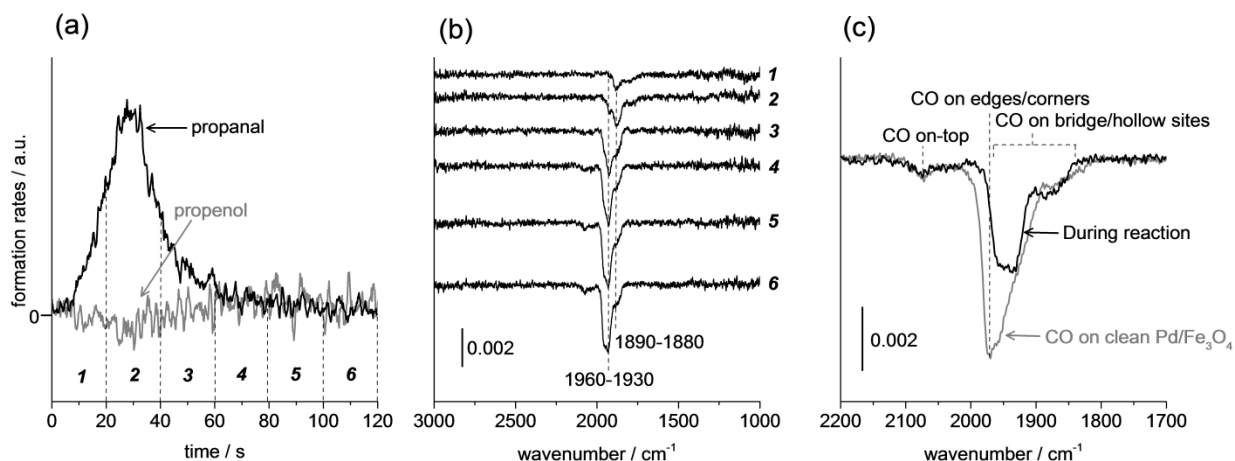maximum at ~30 seconds and then decreases to zero after ~90 seconds.

Figure 4. *Acrolein hydrogenation over 12 nm Pd/Fe₃O₄ at 270 K. (a) Gas-phase formation rates of propanal (black) and propenol (grey). (b) Time-resolved IRAS spectra collected during acrolein hydrogenation. Spectra labeled 1-6 were collected during the corresponding regions labeled 1-6 in (a). (c) Comparison of the IRAS spectrum collected during acrolein hydrogenation over 12 nm Pd/Fe₃O₄ at 270 K (spectrum 6 in (b)) to the IRAS spectrum of CO adsorbed on clean 12 nm Pd/Fe₃O₄.*

The IRAS spectra labeled '1' through '6' in Figure 4(b) were collected during the

corresponding regions labeled in Figure 4(a). All of the bands observed during acrolein

hydrogenation over Pd(111) at 270 K (Figure 2(b)) are absent from the spectra collected during

acrolein hydrogenation over 12 nm Pd particles under the same conditions (Figure 4(b)).

Instead, there are bands in the 1800-1960 cm^{-1} region, which become more intense with

increasing reaction time. These bands are characteristic of CO molecules adsorbed on 12 nm Pd

particles,[9] which are likely formed as a product of acrolein decarbonylation. To demonstrate

that the IR spectra displayed in Figure 4(b) are the result of CO adsorbed on Pd nanoparticles,

Figure 4(c) shows a comparison of the IR spectrum collected after ~100 seconds of acrolein

hydrogenation over 12 nm Pd particles (spectrum labeled '6' in Figure 4(b)) to the IR spectrum

of a saturation coverage of CO on clean 12 nm Pd particles at 300 K. The two spectra are similar

except the spectrum of CO on clean 12 nm Pd particles is more intense at ~1970 cm^{-1}, which is

the position associated with CO adsorbed on edges of Pd particles.[9] This distribution of the IR

intensity is indicative of the (111) facets of the Pd nanoparticles being covered by CO during

acrolein hydrogenation at 270 K and the edges of the nanoparticles being occupied by some

decomposition products that are not detected in our spectra.

The IRAS spectra collected during acrolein hydrogenation over 12 nm Pd particles at 270

K differ from those of Pd(111), which explains the observed differences in the selective

hydrogenation of acrolein over the two surfaces. While over Pd(111), the major species formed

are the oxopropyl spectator species, reaction intermediate propenoxy and the second type of

spectator ethylidine-like species, none of the bands associated with these species were observed

during acrolein hydrogenation over the 12 nm Pd particles. Similar results were observed over 7

nm Pd particles at 270 K (data not shown). These differences in the surface composition under

the reaction conditions are most likely related to the fact that the edges and corners of Pd

nanoparticles readily decompose acrolein to produce CO, which diffuses to the (111) facets and

prevent formation of oxopropyl spectator species.

3.3. Particle size and temperature effects in selective hydrogenation of acrolein over Pd/Fe$_3$O$_4$

In this section, we investigate the effects of particle size and reaction temperature on the

formation of the oxopropyl surface species controlling the selectivity in hydrogenation of

acrolein.

Figure 5(a) shows the rates of propanal and propenol formation during acrolein

hydrogenation over 12 nm Pd particles at 220 K. As expected based on the results obtained for

Pd(111) at this reaction temperature, formation of propenol was negligible over the entire course

of the reaction. The total amount of propanal produced, which was estimated by the integral area

of the propanal production rate, was nearly triple the amount produced at 270 K. The IRAS

spectra collected during acrolein hydrogenation over 12 nm Pd particles at 220 K are displayed

in Figure 5(b). After the first 45 seconds of the reaction (spectrum 1), there are three main bands

in the IRAS spectra that do not change significantly with increasing reaction time. The band at

1855 cm^{-1} is associated with CO molecules adsorbed on facets of the Pd nanoparticles. The band

at 1670 cm^{-1} is associated with the C=O stretching mode in molecular acrolein. The band at

1755 cm^{-1} is associated with the C=O stretching mode of the oxopropyl spectator species.
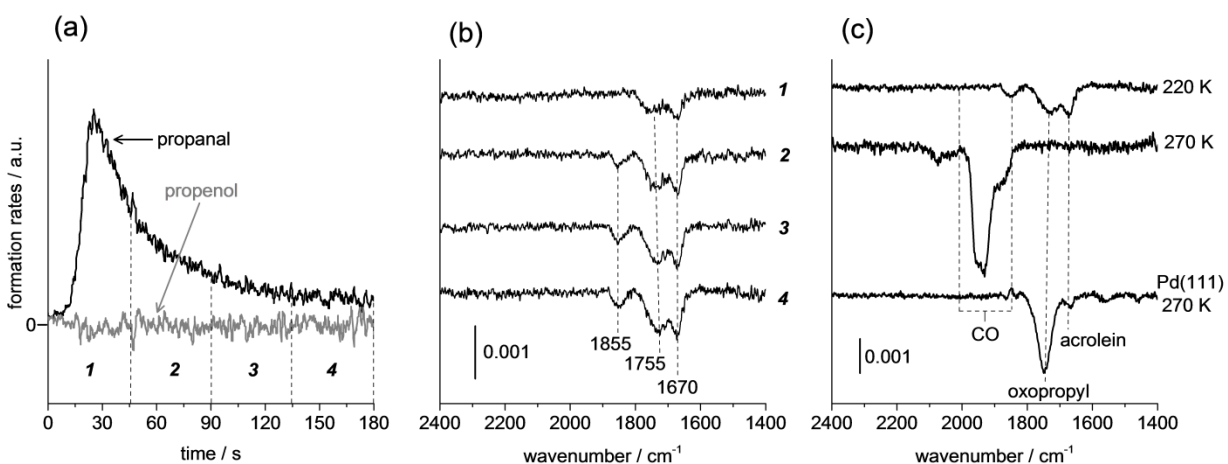

Figure 5. Acrolein hydrogenation over 12 nm Pd/Fe$_3$O$_4$ at 220 K (a) Gas-phase formation rates of propanal (black) and propenol (grey). (b) Time-resolved IRAS spectra collected during acrolein hydrogenation. Spectra labeled 1-4 were collected during the regions labeled 1-4 in (a). (c) Comparison of IRAS spectra collected during acrolein hydrogenation over 12 nm Pd/Fe$_3$O$_4$ at 220 K and 270 K, and over Pd(111) at 270 K.

There are significant differences in the IRAS spectra collected during acrolein

hydrogenation over the 12 nm Pd particles at 220 K as compared to 270 K as evidenced in Figure

5(c). The IRAS spectrum collected during acrolein hydrogenation over Pd(111) at 270 K, which

shows a strong band associated with the oxopropyl species, is also shown in Figure 5(c) for comparison. On the Pd nanoparticles, reduction of the sample temperature from 270 K to 220 K results in a large decrease in the amount of adsorbed CO, and a significant increase in the amount of molecular acrolein (band 1670 cm^{-1}). This observation clearly indicates that the extent of acrolein decomposition on the Pd nanoparticles is greatly reduced by decreasing the sample temperature from 270 K to 220 K. Interestingly, the oxopropyl species which turns Pd(111) selective for C=O bond hydrogenation was observed on the 12 nm Pd particles at 220 K, yet no propenol was detected during acrolein hydrogenation over the 12 nm Pd particles at 220 K. However, since the rate of propenol production over Pd(111) is very low at 220 K (Figure 1), the propenol formation over the Pd nanoparticles is most likely also kinetically hindered at this temperature, even if the activating oxopropyl species is present.

Since we observed oxopropyl spectator species over 12 nm Pd nanoparticles at 220 K, we decided to try slightly higher temperature – 250 K – to test the feasibility of propenol formation. Figure 6(a) shows the formation rates of propanal and propenol during acrolein hydrogenation over 12 nm Pd particles at 250 K. Note that these data were obtained with a lower acrolein flux (0.6x10^{13} molecules/cm^2/s) than the data displayed in Figure 1 (1.5x10^{13} molecules/cm^2/s) for the same particle size and temperature range. Similar to the results obtained at 220 K, the rate of propanal production reaches a maximum at ~30 seconds and then slowly decays to zero after ~100 seconds of acrolein hydrogenation. In contrast to the results at 220 K, however, there is a noticable amount of propenol production over 12 nm Pd particles at 250 K. Following an induction period of ~40 seconds at the beginning of the reaction, the rate of propenol formation increases to a maximum at ~60 seconds and then begins to slowly decay to zero after ~150 seconds. The amount of propenol produced over 12 nm Pd particles at 250 K is also much less

than (~1/30th) the amount produced over Pd(111) at 270 K. However, these results clearly

indicate that propenol formation is possible over 12 nm Pd nanoparticles in a narrow temperature
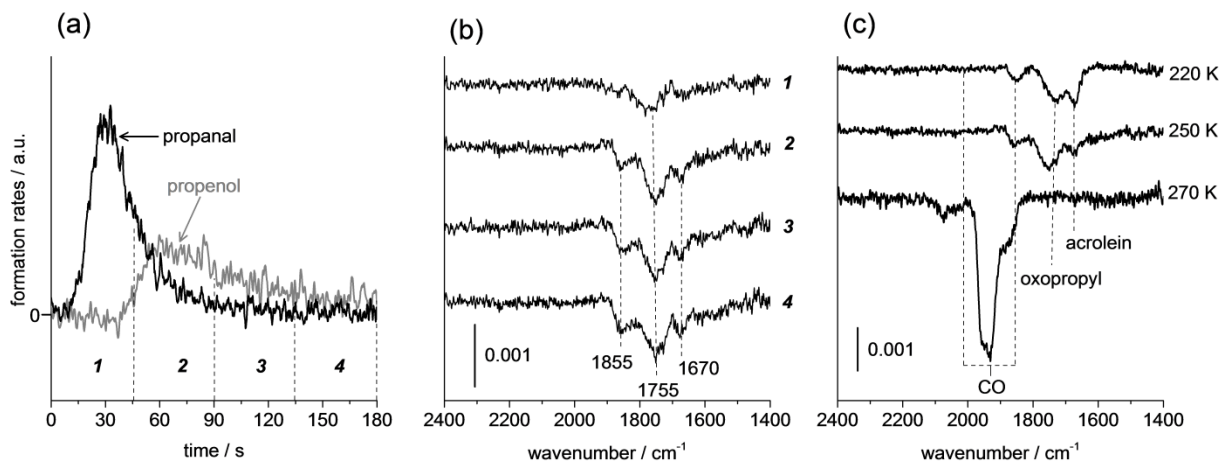
close to 250 K.

Figure 6. *Acrolein hydrogenation over 12 nm Pd/Fe$_3$O$_4$ at 250 K. (a) Gas-phase formation rates of propanal (black) and propenol (grey). (b) Time-resolved IRAS spectra collected during acrolein hydrogenation. Spectra labeled 1-4 were collected during the regions labeled 1-4 in (a). (c) Comparison of IRAS spectra collected during acrolein hydrogenation over 12 nm Pd/Fe$_3$O$_4$ at 220 K, 250 K, and 270 K*

The induction period in the propenol formation rate shown in Figure 6(a) was also

observed during acrolein hydrogenation over Pd(111) at 270 K (Figure 2), and indicates that the

Pd nanoparticles must also accumulate certain amount of acrolein-derivatives prior to the onset

of propenol formation. IRAS spectra obtained during acrolein hydrogenation over 12 nm Pd

particles at 250 K, shown in Figure 6(b), give some insight into the activation process. The

IRAS spectrum collected during the induction period, labeled '1' in Figure 6(b), shows only one

band at 1755 cm^{-1} that is associated with the oxopropyl spectator species (Figure 3), which is

crucial for activation of Pd(111) facets for C=O hydrogenation. The observation of only the

oxopropyl spectator species on both Pd(111) and the 12 nm Pd particles during the induction

period further supports our conclusion that this species activates the Pd surface for propenol formation.

The IRAS spectra collected after the induction period, labeled '2' through '4' in Figure 6(b), show two additional bands at 1855 cm^{-1} and 1670 cm^{-1}. These bands are associated with CO adsorbed on the Pd nanoparticles and molecularly adsorbed acrolein, respectively. Figure 6(c) shows a comparison of the IRAS spectra collected during acrolein hydrogenation over 12 nm Pd particles at 220 K, 250 K, and 270 K. The IRAS spectrum recorded during acrolein hydrogenation over 12 nm Pd particles at 250 K is similar to the one collected at 220 K. The surfaces at 220 K and 250 K are composed of a mixture of molecularly adsorbed acrolein, partially-hydrogenated acrolein species (oxopropyl), and decomposition products (CO). However, increasing the temperature from 250 K to 270 K greatly increases the extent of acrolein decomposition, and, as a result, the surface is nearly saturated with CO. These findings indicate that the composition of the adsorbate's overlayer, thus the reaction pathway of acrolein on Pd nanoparticles, is highly sensitive to the sample temperature, and propenol formation is only possible in a narrow temperature range around 250 K.

In addition to the strong influence of sample temperature on the surface reaction pathway of acrolein on Pd nanoparticles, the nanoparticle size also was found to have a significant influence on its selectivity. Figure 7(a) shows the gas-phase formation rates of propanal and propenol during acrolein hydrogenation over 7 nm Pd particles at 250 K. Similar to the behavior of the 12 nm Pd particles (Figure 6(a)), the propanal formation rate increases from the beginning of the reaction up to a maximum at ~30 seconds, and then decreases to zero after ~90 seconds. In contrast to the 12 nm particles, however, there was no significant propenol formation over the 7 nm particles.
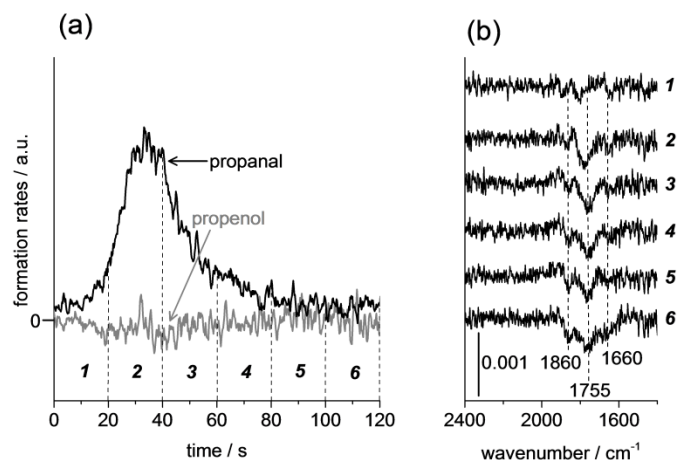
Figure 7. *Acrolein hydrogenation over 7 nm Pd/Fe$_3$O$_4$ at 250 K. (a) Gas-phase formation rates of propanal (black) and propenol (grey). Time-resolved IRAS spectra collected during acrolein hydrogenation. Spectra labeled 1-6 were collected during the regions labeled 1-6 in (a).*

Although there is a significant difference in the selectivity displayed by the 7 nm and the 12 nm particles, the IRAS spectra collected during acrolein hydrogenation over 7 nm particles at 250 K, displayed in Figure 7(b), are similar to the spectra collected over the 12 nm particles under the same reaction conditions (Figure 6(b)). There are three main bands in both sets of spectra at ~1860, ~1755, and ~1660 cm^{-1} which are associated with CO on particle facets, the oxopropyl spectator species, and molecularly adsorbed acrolein, respectively. The intensity of all three of these bands is significantly lower with the 7 nm particles than with the 12 nm particles, which is likely due to the lower concentration of Pd atoms in the 7 nm Pd sample. It is surprising that band at ~1755 cm^{-1}, which we believe is associated with the species that activates the Pd surface for propenol production, is observed over the 7 nm particles at 250 K, yet no propenol formation is observed. It is possible that larger modified domains are more efficient, or that a minimum domain size is required, for propenol production.

We have shown that the selectivity in partial hydrogenation of acrolein is highly sensitive to both the Pd catalyst structure and the temperature. The selectivity towards the desired product propenol increases with increasing Pd particle size, from 0% over 4 and 7 nm particles up to nearly 100% over Pd(111), which is effectively an infinitely large particle. The 12 nm Pd particles were also capable of producing a significant amount of propenol, but only in a narrow temperature range around 250 K. Analysis of the surface species *in-situ* with IRAS allows us to better understand the underlying mechanisms that are responsible for this strong structure and temperature dependence.

Our results suggest that the formation of an oxopropyl spectator species, which results from partial hydrogenation of the C=C bond in acrolein and which has a characteristic vibrational band at 1755 cm^{-1}, turns the Pd(111) surface selective for propenol formation. Propenol formation is not observed over Pd(111) until a critical coverage of the oxopropyl species is achieved, after which the propenol formation rate increases rapidly. This suggests that dense domains of oxopropyl species are required to activated Pd(111) for hydrogenation of the C=O bond in acrolein, although it is not clear how. Several recent studies[16] have shown that organic ligands deposited onto the surfaces of catalysts can enhance selectivity in hydrogenation of multi-functional organic compounds, which can be invoked to understand how oxopropyl acts at the mechanistic level. Three distinct mechanisms by which the organic ligands enhance selectivity have been proposed[16a]: (1) active-site selection, (2) molecular recognition, and (3) steric effects. It is possible that the oxopropyl species creates a geometric confinement on the surface (steric effects), or the C=O group in oxopropyl interacts repulsively with the C=O group in acrolein (molecular recognition), which favors interaction of the C=O group with the catalyst surface.

Formation of the densely packed oxopropyl overlayer is more difficult over Pd nanoparticles because – in contrast to Pd(111) – acrolein decomposes on Pd clusters, which is most likely related to the low-coordinates sites such as the edges and the corners. As a result of the lower surface density of oxopropyl species, the selectivity towards propenol formation is much lower over Pd nanoparticles than over Pd(111). The extent of acrolein decomposition decreases with decreasing temperature, and the oxopropyl species is observed over both 7 nm and 12 nm Pd nanoparticles at 220 K and 250 K. However, significant propenol formation is only observed over 12 nm Pd nanoparticles at 250 K. Therefore, formation of oxopropyl is necessary, but not sufficient, for propenol formation over Pd nanoparticles. Propenol formation is not expected at 220 K because this temperature is too low for significant propenol formation, even over Pd(111). The enhanced selectivity of the 12 nm Pd nanoparticles relative to the 7 nm Pd nanoparticles at 250 K could be most likely related to the formation of densely packed oxopropyl domains over larger (111) terraces of 12-nm sized nanoparticles. Smaller sized terraces of 7- and 4-nm particles might be not large enough to form these densely packed and probably well-ordered oxopropyl overlayers responsible for high selectivity towards propenol. These results demonstrate that the selective hydrogenation of acrolein is highly sensitive to the catalyst structure and temperature because the formation of oxopropyl spectator species, which control the selectivity, is also highly sensitive to the catalyst structure and temperature.

The results from this work provide several promising strategies for rational design of nanoparticle systems for selective propenol formation. For example, it may be possible to selectively poison the edges of Pd nanoparticles with organic ligands to prevent acrolein decomposition. Another possibility is to pre-modify Pd nanoparticles by depositing thioacetic

acid, which has a structure similar to that of oxopropyl, or some other organic ligands in order to mimic the selectivity enhancement produced by oxopropyl species.

4. Conclusions

The selectivity in hydrogenation of acrolein is strongly dependent on both the structure of the Pd catalyst and the reaction temperature. We attribute these effects to the formation of a densely packed overlayer of the oxopropyl species, which controls the selectivity and which is highly sensitive to the catalyst structure and temperature. Near 100% selectivity towards the desired product propenol is observed over Pd(111), but only after a densely packed layer of oxopropyl species was formed (approximately one oxopropyl per four surface Pd atoms) which results from half-hydrogenation of the C=C bond in acrolein. Over Pd nanoparticles with particle sizes ranging from 4 to 12 nm, formation of this oxopropyl layer is much more difficult because acrolein decarbonylates strongly on the Pd nanoparticles, most likely at the edges, thus preventing formation of densely packed layers of oxopropyl, especially on the small Pd clusters. As a result, no propenol formation is observed on 4-7 nm sized nanoparticles. A significant amount of propenol was detected during acrolein hydrogenation over 12 nm Pd nanoparticles, but only in a narrow temperature range around 250 K. These results and the spectroscopically identified surface composition evolving during the reaction suggest that the selectivity towards propenol formation increases with Pd nanoparticle size, most likely because the relative fraction of (111) facets increases with nanoparticle size, allowing more effective formation of densely packed oxopropyl overlayers and diminishing the concentration of the acrolein decomposition products (CO and carbonaceous residues). An effective control over the extent of acrolein decomposition can be achieved by tuning the reaction temperature.

23
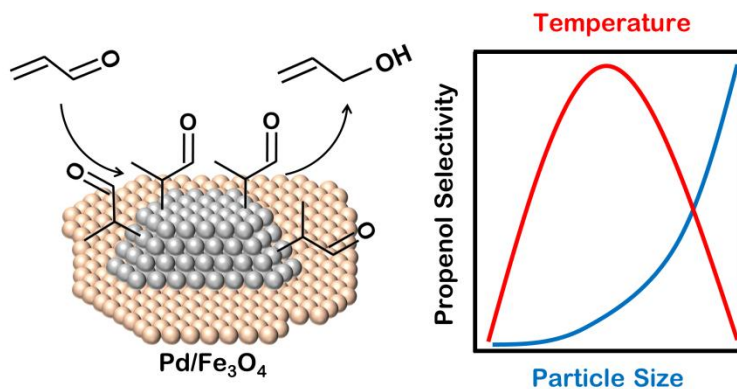
Spectators enhance selectivity: The selectivity towards hydrogenation of C=O in acrolein is enhanced by the formation of oxopropyl spectator species on the surface of Pd model catalysts. Formation of this activating spectator species is highly sensitive to both temperature and particle size.

References

[1]   P. Claus, *Topics in Catalysis* **1998**, *5*, 51-62.

[2]   aJ. C. de Jesus, F. Zaera, *Surface Science* **1999**, *430*, 99-115; bF. Delbecq, P. Sautet, *Journal of Catalysis* **1995**, *152*, 217-236; cK. Brandt, M. E. Chiu, D. J. Watson, M. S. Tikhov, R. M. Lambert, *J. Am. Chem. Soc.* **2009**, *131*, 17286-17290; dH. J. Wei, C. Gomez, J. J. Liu, N. Guo, T. P. Wu, R. Lobo-Lapidus, C. L. Marshall, J. T. Miller, R. J. Meyer, *Journal of Catalysis* **2013**, *298*, 18-26; eM. Bron, D. Teschner, A. Knop-Gericke, B. Steinhauer, A. Scheybal, M. Havecker, D. Wang, R. Fodisch, D. Honicke, A. Wootsch, R. Schlogl, P. Claus, *Journal of Catalysis* **2005**, *234*, 37-47; fM. Bron, D. Teschner, A. Knop-Gericke, F. C. Jentoft, J. Krohnert, J. Hohmeyer, C. Volckmar, B. Steinhauer, R. Schlogl, P. Claus, *Phys. Chem. Chem. Phys.* **2008**, *10*, 7325-7327.

[3]   P. Gallezot, D. Richard, *Catalysis Reviews-Science and Engineering* **1998**, *40*, 81-126.

[4]   K.-H. Dostert, C. P. O'Brien, W. Riedel, A. Savara, W. Liu, M. Oehzelt, A. Tkatchenko, S. Schauermann, *Journal of Physical Chemistry C* **2014**, *118*, 27833-27842.

[5]   aK.-H. Dostert, C. P. O'Brien, F. Ivars-Barcelo, S. Schauermann, H.-J. Freund, *J. Am. Chem. Soc.* **2015**, *137*, 13496-13502; bC. O'Brien, K.-H. Dostert, M. Hollerer, C. Stiehler, F. Calaza, S. Schauermann, S. Shaikhutdinov, M. Sterrer, H. J. Freund, *Faraday Discussions* **2015**.

[6]   aA. Giroir-Fendler, D. Richard, P. Gallezot, in *Studies in Surface Science and Catalysis, Vol. Volume 41* (Eds.: J. B. C. B. D. D. C. M. M. Guisnet, G. Pérot), Elsevier, **1988**, pp. 171-178; bM. L. A. Vonholleben, M. Zucolotto, C. A. Zini, E. R. Oliveira, *Tetrahedron* **1994**, *50*, 973-978; cR. A. Karakhanov, T. I. Odintsova, V. B. Yakovlev, A. P. Rodin, *Reaction Kinetics and Catalysis Letters* **1987**, *33*, 219-221.

[7]   aW. Grunert, A. Bruckner, H. Hofmeister, P. Claus, *Journal of Physical Chemistry B* **2004**, *108*, 5709-5717; bP. Claus, A. Bruckner, C. Mohr, H. Hofmeister, *J. Am. Chem. Soc.* **2000**, *122*, 11430-11439; cC. E. Volckmar, M. Bron, U. Bentrup, A. Martin, P. Claus, *Journal of Catalysis* **2009**, *261*, 1-8; dC. Mohr, H. Hofmeister, J. Radnik, P. Claus, *J. Am. Chem. Soc.* **2003**, *125*, 1905-1911.

[8]   J. Libuda, I. Meusel, J. Hartmann, H. J. Freund, *Review of Scientific Instruments* **2000**, *71*, 4395-4408.

[9]   T. Schalow, B. Brandt, D. E. Starr, M. Laurin, S. K. Shaikhutdinov, S. Schauermann, J. Libuda, H. J. Freund, *Phys. Chem. Chem. Phys.* **2007**, *9*, 1347-1361.

[10]   aW. Weiss, W. Ranke, *Progress in Surface Science* **2002**, *70*, 1-151; bC. Lemire, R. Meyer, V. E. Henrich, S. Shaikhutdinov, H. J. Freund, *Surface Science* **2004**, *572*, 103-114.

[11]   T. Schalow, B. Brandt, D. E. Starr, M. Laurin, S. Schauermann, S. K. Shaikhutdinov, J. Libuda, H. J. Freund, *Catalysis Letters* **2006**, *107*, 189-196.

[12]   P. Maki-Arvela, J. Hajek, T. Salmi, D. Y. Murzin, *Appl. Catal. A-Gen.* **2005**, *292*, 1-49.

[13]   aJ. C. de Jesús, F. Zaera, *Surf. Sci.* **1999**, *430*, 99-115; bL. E. Murillo, J. G. Chen, *Surf. Sci.* **2008**, *602*, 919-931; cF. Bournel, C. Laffon, P. Parent, G. Tourillon, *Surf. Sci.* **1996**, *359*, 10-16.

[14]   aN. B. Colthup, L. H. Daly, S. E. Wiberley, in *Introduction to Infrared and Raman Spectroscopy (Third Edition)*, Academic Press, San Diego, **1990**, pp. 289-325; bB. Mecke, K. Noack, *Spectrochimica Acta* **1958**, *12*, 391-393.

[15]   F. Zaera, *Langmuir* **1996**, *12*, 88-94.

[16]   aC. A. Schoenbaum, D. K. Schwartz, J. W. Medlin, *Accounts of Chemical Research* **2014**, *47*, 1438-1445; bS. H. Pang, C. A. Schoenbaum, D. K. Schwartz, J. W. Medlin, *ACS Catal.* **2014**, *4*, 3123-3131; cS. H. Pang, J. W. Medlin, *J. Phys. Chem. Lett.* **2015**, *6*, 1348-1356; dK. R. Kahsar, D. K. Schwartz, J. W. Medlin, *J. Am. Chem. Soc.* **2014**, *136*, 520-526.